Field-Effect Mobility of Organic Polymer Thin-Film Transistors

Michael C. Hamilton, Sandrine Martin, and Jerzy Kanicki*

Department of Electrical Engineering and Computer Science, The University of Michigan, Ann Arbor, Michigan 48109

We present a method of extracting the field-effect mobility from the transfer characteristics of organic polymer thin-film transistors (OP-TFTs), in both the linear and saturation regimes, by accounting for the dependence of the mobility on the gate bias, which translates to a dependence on the accumulated density of majority charge carriers in the channel. This method is compared to the commonly used extraction methods, which are based on the standard MOSFET square-law drain current equations that do not account for the variation of mobility with the applied gate bias. We show that by using the standard MOSFET equations, the extracted field-effect mobility can be significantly overestimated. We also demonstrate the use of the proposed method to extract the field-effect mobility at different measurement temperatures and present the dependence of the extracted parameters on temperature.

I. Introduction

The electrical performance of organic electronic devices such as organic thin-film transistors (O-TFTs) has steadily increased over the past several years.[1−5] This increase can be attributed to the development of high-quality organic semiconductors and to the engineering of device structures and fabrication methods, as well as to the progress made in explaining the underlying physics of organic materials and devices. One important factor in the development of this class of devices is the ability to reliably compare the various performance parameters (i.e., field-effect mobility, threshold voltage, and ON/OFF ratio) extracted for different devices and found by different research groups. In this paper, we will discuss the methods used to extract the field-effect mobility from the transfer characteristics of organic polymer thin-film transistors (OP-TFTs).

In the past, several groups have examined the field-effect mobility in OP-TFTs from various theoretical perspectives. These studies were based on either the variable-range hopping (VRH) model[6−8] or on the multiple trapping and release (MTR) model[9,10] For the case of VRH, the transport of charge carriers occurs within organic molecules by hopping (or tunneling) from one localized state to another, either over a short distance with a relatively high activation energy or over a longer distance with a smaller activation energy. In the MTR model, the charge carriers move within organic molecules from localized states to delocalized states by thermal activation. Charge transport occurs through the delocalized states until the carriers are trapped into another localized state, and so on. The derived analytical expressions were shown to agree well with the experimentally determined gate bias and temperature dependence, and the validity of each model to various organic molecular systems (i.e., well organized small molecule systems versus amorphous polymer systems) is still under debate.
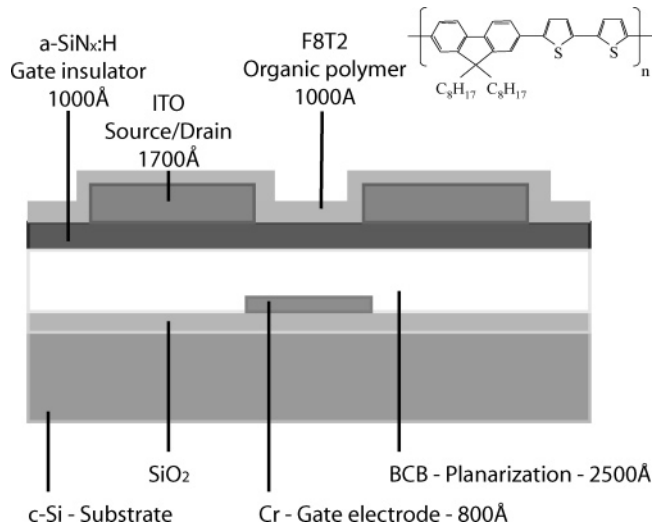
Other groups have studied the effect of various device fabrication methods on the field-effect mobility. It was observed that the field-effect mobility has a significant dependence on the morphology and ordering of the molecules in the thin-film (for small molecules and polymers). The ordering of the molecules can be controlled by the deposition temperature and rate for vacuum-deposited small molecules,[11−13] by the solvent used for deposition from solution,[14,15] and by mechanical treatment of the substrate before the deposition of the organic semiconductor. Furthermore, it should be noted that the dependence of the charge carrier mobility on

* To whom correspondence should be addressed. E-mail: kanicki@eecs.umich.edu.

(1) Horowitz, G. *Adv. Mater.* **1998**, *10*, 365−377.
(2) Dimitrakopoulos, C. D.; Mascaro, D. J. *IBM J. Res. Dev.* **2001**, *45*, 11−27.
(3) Jackson, T. N.; Lin, Y.; Gundlach, D. J.; Klauk, H. *IEEE J. Select. Topics Quantum Electron.* **1998**, *4*, 100−104.
(4) Martin, S.; Nahm, J. Y.; Kanicki, J. *J. Electron. Mater.* **2002**, *31*, 512−519.
(5) Martin, S.; Hamilton, M. C.; Kanicki, J. *J. SID* **2003**, *11*, 543−549.
(6) Brown, A. R.; Jarrett, C. P.; deLeeuw, D. M.; Matters, M. *Synth. Met.* **1997**, *88*, 37−55.
(7) Vissenberg, M. C. J. M.; Matters, M. *Philos. Rev. B* **1988**, *57*, 12964−12967.
(8) Paasch, G.; Lindner, T.; Scheinert, S. *Synth. Met.* **2002**, *132*, 97−104.

(9) Horowitz, G.; Hajlaoui, R.; Bourguiga, R.; Hajlaoui, M. *Synth. Met.* **1999**, *101*, 401−404.
(10) Horowitz, G. *Synth. Met.* **2003**, *138*, 101−105.
(11) Garnier, F.; Horowitz, G.; Fichou, D.; Yassar, A. *Synth. Met.* **1996**, *81*, 163−171.
(12) Laquindanum, J. G.; Katz, H. E.; Lovinger, A. J.; Dodabalapur, A. *Chem. Mater.* **1996**, *8*, 2542−2544.
(13) Gundlach, D. J.; Lin, Y. Y.; Jackson, T. N.; Nelson, S. F.; Schlom, D. G. *IEEE Electron Device Lett.* **1997**, *18*, 87−89.
(14) Geens, W.; Tsamouras, D.; Poortmans, J.; Hadziioannou, G. *Synth. Met.* **2001**, *122*, 191−194.
(15) Geens, W.; Shaheen, S. E.; Wessling, B.; Brabec, C. J.; Poortmans, J.; Sariciftci, N. S. *Org. Electron.* **2002**, *3*, 105−110.

4700 *Chem. Mater., Vol. 16, No. 23, 2004*

Hamilton et al.

Figure 1. Cross-section of OP-TFT device structure and chemical structure of F8T2.

Figure 2. Typical OP-TFT linear regime transfer characteristics. Arrows indicate direction of measurement.

the applied gate bias seems to arise from the variation of the mobility with carrier density in the channel.[9,10,16] The density of charge carriers in the channel is controlled by the applied gate bias (i.e., accumulation of holes in p-channel devices), therefore, this translates into the observed dependence of the carrier mobility with the applied gate bias.

Due to the dependence of the mobility on applied gate bias, it has often been observed that the OP-TFT transfer characteristics do not always exhibit an ideal linear behavior with gate-to-source bias, at low drain-to-source voltage.[17,18] In this paper, we present a tractable method of extracting the field-effect mobility from the transfer characteristics of OP-TFTs, in both the linear and saturation regimes. This method is based on the commonly used MOSFET drain current equations with a modification to allow the dependence on the applied gate bias to be taken into account. Using this method, we show that the field-effect mobility extracted using the standard equations can be significantly overestimated, giving results that may be unreliable.[19] This method is then used to extract the field-effect mobility and related parameters from the transfer characteristics at different temperatures, and the dependence of these parameters on temperature is presented.

II. Experimental Section

A. Device Structure. A schematic cross-section of the OP-TFT that we have used in this study is shown in Figure 1. The device is in an inverted, defined-gate, gate-planarized, coplanar thin-film transistor configuration and has been described in more detail elsewhere.[4,5,20,21] Indium tin oxide (ITO) was used for the source and drain contacts, benzocyclobutene (BCB) was used as the gate-planarization layer and also functions as a gate insulator, PECVD hydrogenated
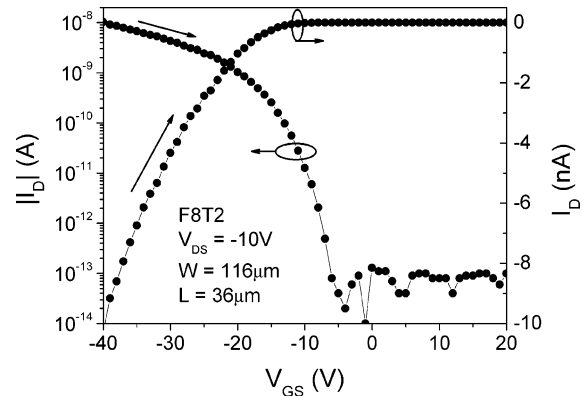
amorphous silicon nitride (a-SiN:H) was used as a second gate insulator layer, and chromium (Cr) was used for the patterned gate electrode. The patterned gate electrode provides enhanced device performance by reducing parasitic leakage currents outside of the intended channel of the device. The BCB gate-planarization layer provides a smooth surface, such that better step-coverage and adhesion of subsequently deposited layers (i.e., a-SiN:H and ITO) is achieved. The devices were fabricated on a silicon substrate with a thick, thermally grown silicon dioxide layer to facilitate processing in standard microelectronic fabrication equipment and provide electrical isolation of the devices. We used a 1 wt % solution of the organic semiconductor F8T2 [poly(9,9-dioctylfluorene-*co*-bithiophene)] alternating copolymer from Dow Chemical Company (chemical structure shown in Figure 1) dissolved in either xylenes or mesitylenes at a temperature of approximately 50 °C. The heated solution was deposited by spin-coating and cured in a vacuum oven at 90 °C, providing a uniform film with an approximate thickness of 1000 Å. Samples are stored in air, at room temperature, and with yellow ambient light.

B. Measurement Setup. The transfer characteristics (drain current versus gate-to-source voltage, $I_D - V_{GS}$) of the OP-TFT were measured in the dark, at various temperatures, using a Karl Suss PM8 probe station, and an HP4156 semiconductor parameter analyzer controlled by Interactive Characterization Software (Metrics). The transfer characteristic measurements performed in this study were measured from the strong accumulation (i.e., ON-state) to the OFF-state, as is commonly done. Transfer characteristic measurements performed in this manner provide more reliable and repeatable results, since any nonideal effects that depend on the applied gate bias, which would accumulate for the case of measurement from the OFF-state to the ON-state, occur at the start of the measurement. A Signatone QuiteTemp temperature controller and hot-chuck were used to control the temperature of the devices between 10 and 80 °C. All measurements were performed in ambient atmosphere.

III. Extraction Methods and Discussion

OP-TFTs based on F8T2 exhibit p-channel field-effect transistor action as can be seen from the typical linear regime transfer characteristics shown in Figure 2. As stated above, the OP-TFT transfer characteristics at low drain voltage do not always exhibit a perfectly linear behavior with applied gate bias, above the threshold voltage, as in the case of ideal c-Si MOSFETs. The typical transfer characteristics of an OP-TFT are shown

(16) Tanase, C.; Meijer, E. J.; Blom, P. W. M.; deLeeuw, D. M. *Org. Electron.* **2003**, *4*, 33−37.

(17) Necliudov, P. V.; Shur, M. S.; Gundlach, D. J.; Jackson, T. N. *J. Appl. Phys.* **2000**, *88*, 6594−6597.

(18) Horowitz, G.; Hajlaoui, R.; Fichou, D.; Kassmi, A. E. *J. Appl. Phys.* **1999**, *85*, 3202.

(19) Detcheverry, C.; Matters, M. In *Proceedings of European Solid State Device Research Conferences, 2000*; Seguier: Paris, 2000; pp 328−3311.

(20) Martin, S.; Kanicki, J. In *Proceedings of the International Display Research Conference 2002*; Le Club Visu Society for Information Display-France: Brive La Gaillarde, France, 2002; pp 25−28.

(21) Hamilton, M. C.; Martin, S.; Kanicki, J. In *Proceedings of the International Display Research Conference 2003*; Society for Information Display: San Jose, CA, 2003; pp 14−17.
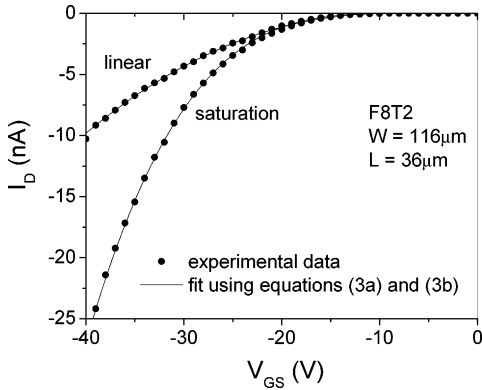
Figure 3. OP-TFT transfer characteristics in the linear and saturation regimes. Symbols represent experimental data, and solid lines show fits to eqs 3a and 3b.

in Figures 2 and 3. The deviation from the ideal c-Si MOSFET behavior has also been observed in a-Si:H TFTs[22-25] where it has been associated with dispersive transport of the charge carriers (electrons) in a-Si:H.[25,26] In general, in amorphous and other low-mobility solids (including organic polymers), the movement of an injected pulse of charges in a steady electric field produces a completely smeared-out drift of the pulse. This is due to heavy trapping of the charge carriers and the slow release from the traps under thermal excitation. In such a case, it is difficult to define the transit time of any particular charge carrier. Instead, the time dependence of the current is described by a power-law:

$$I(t) \propto t^{-s}, \ (0 < s < 2) \qquad (1)$$

where t is time and s is a material-dependent parameter related to the dispersive nature of the transport mechanisms. This type of behavior is known as dispersive carrier transport in disordered materials.

A. Linear and Saturation Regime. To accommodate dispersive carrier transport, we must modify the standard MOSFET equations in the linear and saturation regimes:[27]

$$I_{\mathrm{D}}^{\mathrm{lin}} = -\mu_{\mathrm{FElin}} C_{\mathrm{ins}} \frac{W}{L} (V_{\mathrm{GS}} - V_{\mathrm{Tlin}}) V_{\mathrm{DS}} \qquad (2a)$$

$$I_{\mathrm{D}}^{\mathrm{sat}} = -\mu_{\mathrm{FEsat}} C_{\mathrm{ins}} \frac{W}{2L} (V_{\mathrm{GS}} - V_{\mathrm{Tsat}})^2 \qquad (2b)$$

where μ_{FElin} is the linear regime field-effect mobility, μ_{FEsat} is the saturation regime field-effect mobility, C_{ins} is the gate insulator capacitance per unit area, W is the channel width of the device, L is the channel length of the device, V_{GS} is the applied gate-to-source bias, V_{Tlin} is the threshold voltage in the linear regime, V_{Tsat} is the threshold voltage in the saturation regime, and V_{DS} is the applied drain-to-source bias. Further details of the required modifications can be found in the Appendix.

(22) Merckel, G.; Rolland, A. *Solid-State Electron.* **1996**, *39*, 1231.
(23) Leroux, T. *Solid-State Electron.* **1986**, *29*, 47–58.
(24) Kishida, S.; Naruke, Y.; Uchida, Y.; Matsumura, M. *Jpn. J. Appl. Phys.* **1983**, *22*, 511–517.
(25) Martin, S.; Kanicki, J.; Ugai, Y. In *Proceedings of the International Display Research Conference 1999*; VDE Verlag GMBH: Berlin, Germany, 1999; pp 45–48.
(26) Tiedje, T.; Rose, A. *Solid State Commun.* **1981**, *37*, 49–52.
(27) Pierret, R. F. *Semiconductor Device Physics*; Addison-Wesley: Reading, MA, 1996.

Table 1. Fitting Parameters Used for the Transfer Characteristics Shown in Figure 3

	linear regime	saturation regime
W/L	116/36	116/36
C_{ins} (F/cm^2)	7.5×10^{-9}	7.5×10^{-9}
μ_{FElin0} and μ_{FEsat0} cm^2/V$^\gamma$s	3×10^{-5}	3.5×10^{-6}
μ_{FE} (cm^2/Vs) at $V_{\mathrm{GS}} - V_{\mathrm{T}} = -25$ V	1×10^{-3}	2×10^{-3}
γ	2.1	2.9
T_0 (K)	465	585
V_{Tlin} and V_{Tsat} (V)	-9	-3.3

The modified linear and saturation regime equations, which include an additional parameter, γ, associated with the nonlinearity of the device transfer characteristic for low V_{DS} are given below[22-25]

$$I_{\mathrm{D}}^{\mathrm{lin}} = -\mu_{\mathrm{FElin0}} C_{\mathrm{ins}} \frac{W}{L} (V_{\mathrm{GS}} - V_{\mathrm{Tlin}})^\gamma V_{\mathrm{DS}} \qquad (3a)$$

$$I_{\mathrm{D}}^{\mathrm{sat}} = -\mu_{\mathrm{FEsat0}} C_{\mathrm{ins}} \frac{W}{(\gamma + 1)L} (V_{\mathrm{GS}} - V_{\mathrm{Tsat}})^{\gamma+1} \qquad (3b)$$

where μ_{FElin0} and μ_{FEsat0} are fitting parameters associated with the field-effect mobility of the device in the linear and saturation regimes, respectively, and the other parameters are described above. We should note that the unit of μ_{FElin0} and μ_{FEsat0} is not necessarily cm^2/Vs, but cm^2/V$^\gamma$s.

The physical significance of γ in a-Si:H has often been expressed by

$$\gamma = 2\frac{T_0}{T} - 1 \qquad (4)$$

where T_0 is the characteristic temperature of the inorganic semiconductor density-of-states distribution around the position of the Fermi level.[18,24] The equation is valid for $T < T_0$. In a-Si:H TFTs (n-channel devices), T_0 is the characteristic temperature (slope) of the conduction band tail. The nonideal situation of $\gamma > 1$ is associated with a high density of conduction band tail states, which can be attributed to variations of the Si–Si bond angles and distances in the amorphous semiconductor. We have also previously demonstrated for a-Si:H TFTs[28] that γ can be significantly underestimated in cases of nonnegligible source and drain series resistances. Indeed, $\gamma = 1$ can be observed for a TFT with both a high density of conduction band tail states and high source and drain series resistances.

To fit the OP-TFT experimental data in the linear and saturation regimes over a wide gate voltage range, shown in Figure 3, we used eqs 3a and 3b with the fitting parameters summarized in Table 1. The physical significance of γ values larger than one in organic devices has not yet been fully explained. However, the authors believe that, following amorphous semiconductor theory, it can also be associated with an energy-dependent, high density of states around the Fermi level position caused by residual disorder in the locally self-organized polymer film. As the carrier concentration increases, localized defect states are filled and the Fermi level approaches a region of the density of states of more extended electronic states with higher mobility. Indeed,

(28) Martin, S.; Feillens, Y.; Kanicki, J. In *Conference Record of the 20th International Display Research Conference*; Society for Information Display: San Jose, CA, 2000; pp 127–130.

the gate voltage dependence of the OP-TFT field-effect mobility has already been connected to the characteristic temperature of the semiconductor density-of-states distribution around the position of the Fermi level, T_0.[7] As stated above, when the OP-TFT parameter extraction is performed using eq 3a, the unit of μ_{FElin0} and μ_{FEsat0} is not cm²/Vs, but cm²/V$^\gamma$s, and eq 3a is therefore used only to extract γ.

Alternatively, it is also possible to rewrite eqs 3a and 3b as

$$I_D^{\text{lin}} = -\mu_{\text{FElin0}}(V_{GS} - V_{\text{Tlin}})^{\gamma-1}C_{\text{ins}}\frac{W}{L}(V_{GS} - V_{\text{Tlin}})V_{DS} \quad (5a)$$

$$I_D^{\text{sat}} = -\mu_{\text{FEsat0}}(V_{GS} - V_{\text{Tlin}})^{\gamma-1}C_{\text{ins}}\frac{W}{(\gamma+1)L} \times$$
$$(V_{GS} - V_{\text{Tsat}})^2 \quad (5b)$$

which become

$$I_D^{\text{lin}} = -\mu_{\text{FElin}}(V_{GS})C_{\text{ins}}\frac{W}{L}(V_{GS} - V_{\text{Tlin}})V_{DS} \quad (6a)$$

$$I_D^{\text{sat}} = -\mu_{\text{FEsat}}(V_{GS})C_{\text{ins}}\frac{W}{(\gamma+1)L}(V_{GS} - V_{\text{Tsat}})^2 \quad (6b)$$

with

$$\mu_{\text{FElin}}(V_{GS}) = \mu_{\text{FElin0}}(V_{GS} - V_{\text{Tlin}})^{\gamma-1} \quad (7a)$$

$$\mu_{\text{FEsat}}(V_{GS}) = \mu_{\text{FEsat0}}(V_{GS} - V_{\text{Tsat}})^{\gamma-1} \quad (7b)$$

Equations 6a and 6b are very similar to the standard MOSFET eqs 2a and 2b in the linear and saturation regimes, but contain the gate voltage dependence of the field-effect mobility. It is therefore incorrect to extract μ_{FElin} from eq 2a or μ_{FEsat} from eq 2b, as it is commonly done for the MOSFET, because of the gate voltage dependence of the field-effect mobility. As it has been pointed out previously,[19] doing so would overestimate the field-effect mobility of the device by a factor γ in the linear regime and by $(\gamma + 1)/2$ in the saturation regime, as indicated by the equations below. Using eq 2a or 2b, the field-effect mobility is sometimes extracted using the following equation:

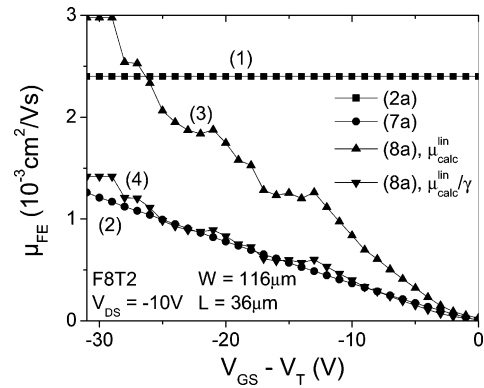$$\mu_{\text{calc}}^{\text{lin}} = \frac{1}{V_{DS}C_{\text{ins}}W/L}\left(\frac{dI_D^{\text{lin}}}{dV_{GS}}\right) \quad (8a)$$

$$\mu_{\text{calc}}^{\text{sat}} = \frac{1}{C_{\text{ins}}W/2L}\left(\frac{d\sqrt{|I_D^{\text{sat}}|}}{dV_{GS}}\right)^2 \quad (8b)$$

with

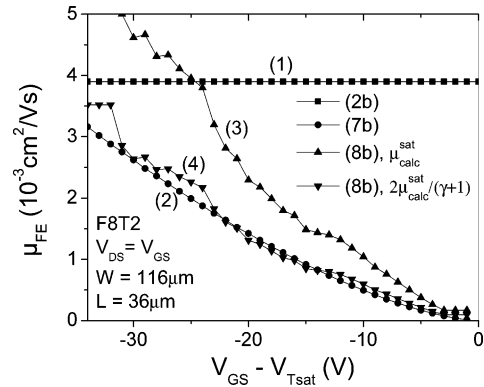$$\frac{dI_D^{\text{lin}}}{dV_{GS}} = \mu_{\text{FElin}}C_{\text{ins}}\frac{W}{L}V_{DS} \quad (9a)$$

$$\frac{d\sqrt{|I_D^{\text{sat}}|}}{dV_{GS}} = \sqrt{\mu_{\text{FEsat}}C_{\text{ins}}\frac{W}{L}} \quad (9b)$$

However, if the field-effect mobility is gate voltage dependent, eqs 2a and 2b have to be replaced by eq 3a

Figure 4. Comparison of the results of several extraction methods used to find the OP-TFT field-effect mobility of the same device as used in Figure 3, in the linear regime.

Figure 5. Comparison of the results of several extraction methods used to find the OP-TFT field-effect mobility of the same device as used in Figure 3, in the saturation regime.

or 6a and eq 3b or 6b, respectively. In such a case, the field-effect mobility expression becomes

$$\mu_{\text{calc}}^{\text{lin}} = \gamma\mu_{\text{FElin0}}(V_{GS} - V_{\text{Tlin}})^{\gamma-1} \quad (10a)$$

$$\mu_{\text{calc}}^{\text{sat}} = \left(\frac{\gamma+1}{2}\right)\mu_{\text{FEsat0}}(V_{GS} - V_{\text{Tsat}})^{\gamma-1} \quad (10b)$$

or

$$\mu_{\text{calc}}^{\text{lin}} = \gamma\mu_{\text{FElin}}(V_{GS}) \quad (11a)$$

$$\mu_{\text{calc}}^{\text{sat}} = \left(\frac{\gamma+1}{2}\right)\mu_{\text{FEsat}}(V_{GS}) \quad (11b)$$

where:

$$\mu_{\text{FElin}}(V_{GS}) = \mu_{\text{FElin0}}(V_{GS} - V_{\text{Tlin}})^{\gamma-1} \quad (12a)$$

$$\mu_{\text{FEsat}}(V_{GS}) = \mu_{\text{FEsat0}}(V_{GS} - V_{\text{Tsat}})^{\gamma-1} \quad (12b)$$

These equations clearly indicate that the OP-TFT field-effect mobility can be overestimated if the parameter extraction is not done properly. These observations are illustrated in Figures 4 and 5 where we have plotted the field-effect mobility in the linear regime and saturation regime, respectively, extracted by the different methods described here. (1) Conventional value extracted from experimental data using eq 2a or 2b, the standard MOSFET drain current equations in the linear and saturation regimes. (2) Values calculated using eq 7a or 7b and the fitting parameters from Table 1. (3)

Values extracted from experimental data using eq 8a or 8b, i.e., $\mu^{\text{lin}}_{\text{calc}}$ or $\mu^{\text{sat}}_{\text{calc}}$.

(4) Values extracted from experimental data using eq 8a or 8b and taking into account γ; i.e., $\mu^{\text{lin}}_{\text{calc}}/\gamma$ or $\mu^{\text{sat}}_{\text{calc}}/\left(\frac{\gamma+1}{2}\right)$.

Note that, as shown in Figures 4 and 5, curves (1) and (3) show significantly overestimated values of the field-effect mobility in both linear and saturation regime. For the case of curve (1), the extraction using the standard MOSFET equations, which ignore the gate bias dependence of the mobility, the extracted mobility is constant with applied gate bias, as shown in the figures. The difference in the results from each method is less significant for large values of the gate bias. On the other hand, curves (2) and (4) are very similar and increase with gate bias, as expected from the discussion above. Therefore, it is critical to keep in mind that when the conventional field-effect mobility extraction method (i.e., using eq 2a or 2b) is applied to OP-TFTs, the values found for the field-effect mobility can be significantly overestimated. We can also conclude that the methods used to extract curves (2) and (4) are the most appropriate for OP-TFTs, and allow a more reliable comparison of the electrical performance of different devices and materials.

In general, the behavior of the mobility for the case of devices based on disordered materials (i.e., OP-TFTs based on F8T2) is different from the case of devices based on crystalline materials (i.e., MOSFETs based on c-Si) because of the nature of the density of states, near the position of the Fermi level, through which the carriers move. Crystalline materials are characterized by well-defined, delocalized transport bands separated by an energy gap that is nearly devoid of localized states, resulting in a mobility that has negligible dependence on the applied gate bias. Whereas in disordered materials, the delocalized transport bands are not well defined and there exists a significant density of localized states in the energy gap. This results in a field-effect mobility that has a significant dependence on the applied gate bias, since the region of the density of states, through which the charge carriers are transported, changes with the applied gate bias.

B. Temperature Dependence of OP-TFT Electrical Characteristics. We have used this extraction method on OP-TFT transfer characteristic data taken at different temperatures ranging from 10 to 80 °C, as shown in Figure 6. It should be noticed that we have used different devices for these measurements. In Figure 6, we see that the OFF-state drain current is significantly affected by the temperature of the device, and increases from approximately 5×10^{-13} A to 5×10^{-12} A as the temperature is increased from 10 to 80 °C. Also, note that the subthreshold slope of the transfer characteristics (i.e., the slope of the semilog plots in the transition regime from the OFF-state to the ON-state) does not appear to be affected by the temperature, signifying that the region of the density of states of the organic semiconductor near the Fermi level is not significantly altered. In Figure 6, the symbols represent the experimental data and the lines show fits of the linear plots using eq 3a. From the fits, we extracted the linear regime field-effect mobility μ_{FElin0}, linear regime
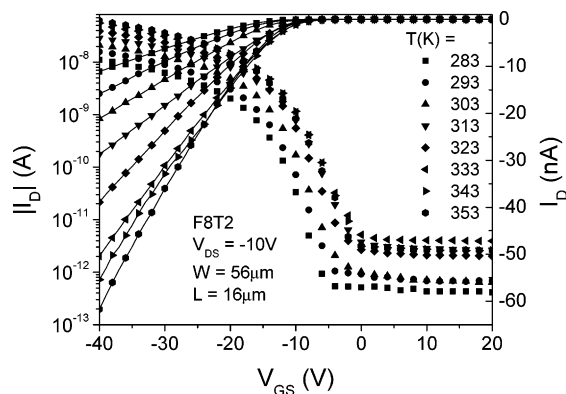
Figure 6. Linear regime transfer characteristics of an OP-TFT measured at different temperatures between 10 and 80 °C. The symbols correspond to experimental data, and the lines correspond to fits using eq 3a.
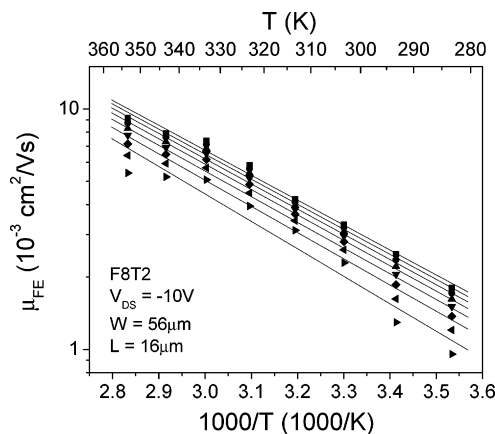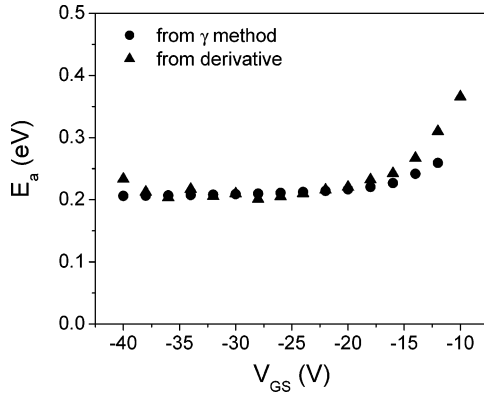

Figure 7. Dependence of the OP-TFT field-effect mobility on temperature, taken from the data shown in Figure 6 at different gate biases. Symbols are experimental data, and straight lines are the fits to an Arrhenius relationship, giving the activation energy (E_a) of the field-effect mobility.

threshold voltage V_{Tlin}, and gamma parameter from the data of Figure 6 at different temperatures. Then, using eq 7a, we calculated μ_{FElin} as a function of applied gate bias for each temperature. The field-effect mobility increases with gate bias, as expected, and the temperature dependence of the field-effect mobility at different applied gate biases is shown in Figure 7. The fit of μ_{FElin} with temperature is an Arrhenius relationship of the form

$$\mu_{\text{FElin}} = \mu^*_{\text{FE}} e^{-E_a/kT} \qquad (13)$$

where μ^*_{FE} is the pre-exponent factor of this mobility and has a value of approximately 10 cm²/V here. The fit is excellent up to approximately 80 °C and we can see that, as expected, the field-effect mobility is activated in temperature. In Figure 8, we present the thermal activation energy E_a of the field-effect mobility as a function of applied gate bias. These data were taken from the mobility data found using methods (2) and (4), described above. From this figure, we see that E_a is constant at a value of approximately 0.2 eV for high applied gate biases ($|V_{\text{GS}}| \gtrsim |V_{\text{T}}|$) and increases for lower gate biases. Similar results were obtained by others and have been associated with the filling of low-lying localized electronic states by the accumulated charges as the gate bias is increased.[7]

Figure 8. Activation energy of the OP-TFT field-effect mobility as a function of applied gate bias, found from the data shown in Figure 7.
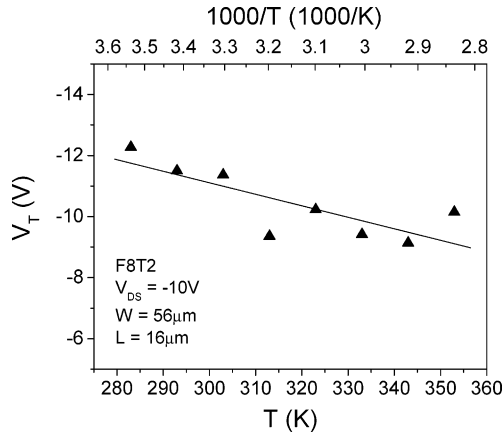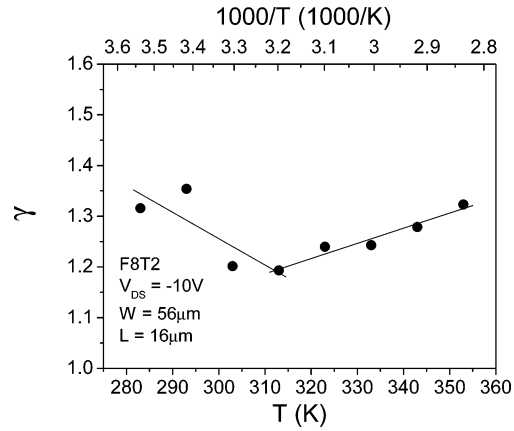

Figure 9. Dependence of the OP-TFT threshold voltage on temperature, extracted from the data shown in Figure 6. Symbols are experimental data, and the straight line is the linear fit which serves as a guide to the eye.

Furthermore, the dependence of the threshold voltage, extracted from Figure 6 using eq 3a, on temperature is shown in Figure 9, and we can see that the threshold voltage decreases slightly with increasing temperature, at a rate of approximately 0.04 V/K over the range of temperature we used here. We present the temperature dependence of γ, found from Figure 6 using eq 3a, in Figure 10. We can see from this figure that γ has a value significantly larger than unity and has a more complex dependence on temperature. The observed temperature dependence is not the expected result that should follow from eq 4. At the lower temperatures, below 40 °C, γ decreases with temperature, as expected. However, at higher temperatures, above 40 °C, the dependence on temperature is reversed and reduced. Though these results were reproduced several times, further investigation of the dependence of γ on temperature is needed.

IV. Conclusion

We have described a method that can be used to reliably extract and compare the field-effect mobility from the transfer characteristics of OP-TFTs. This method is based on the modification of the standard MOSFET equations to include the gate bias dependence of the charge carrier mobility, which can more physically be described as a dependence on the charge carrier density in the channel. We have shown that the use of the standard MOSFET equations to extract the mobility

Figure 10. Dependence of the OP-TFT gamma parameter on temperature, extracted from the data shown in Figure 6. Symbols are experimental data, and the straight lines are linear fits to the corresponding sections of the gamma data and serve as guides to the eye.

can give significantly overestimated results, in both the linear and saturation regimes, and this should be kept in mind when comparing the electrical performance of devices evaluated in this manner. The proposed method was used to extract the field-effect mobility from the transfer characteristics measured at different temperatures and the temperature dependence of the relevant parameters was presented. We observed that the field-effect mobility was thermally activated, with an activation energy (E_a) that depends on the applied gate bias and has a value of approximately 0.2 eV. These results agree with previously published results, demonstrating the validity of the OP-TFT parameter extraction method described in this paper.

Appendix

A general expression for the drain current has been derived by Merckel et al. from Kishida and Leroux:[22−24]

$$I_D = - \mu_{FE} C_{ins} \frac{W}{L} \frac{1}{\gamma + 1}[(V_{GS} - V_T)^{\gamma+1} - (V_{GS} - V_T - V_{DS})^{\gamma+1}] \quad (14)$$

The right side of eq 14 can be series expanded in V_{DS} to the second order to give the linear regime drain current as

$$I_D = - \mu_{FE} C_{ins} \frac{W}{L}(V_{GS} - V_T)^{\gamma-1} \times \left[(V_{GS} - V_T)V_{DS} - \frac{\gamma}{2}V_{DS}^2\right] \quad (15)$$

For low V_{DS}, $\gamma/2$ V_{DS}^2 becomes negligible and eq 15 reduces to eq 3a.

For the saturation regime (i.e., $V_{DS} = V_{GS} - V_T$), eq 14 becomes eq 3b.